ELSEVIER

Journal of Nuclear Materials 266–269 (1999) 906–910

journal of nuclear materials

Effect of gyro-motion of incident ions on inboard–outboard asymmetry in divertor plasmas

Michiya Shimada *, Tihiro Ohkawa [1]

Naka Fusion Research Establishment, Japan Atomic Energy Research Institute, Large Tokamak Experiment Divison II, Mukoyama, Naka-machi, Naka-gun, Ibaraki-ken 311-01, Japan

Abstract

In–out asymmetry of divertor plasmas is observed in many experiments. In single-null divertor configuration, more power is deposited on the electron side, and for the particle flux and electron pressure, ion side is favored over the electron side. Switching toroidal field reverses the in–out asymmetry. In this paper, we point out a possible cause of this asymmetry. The ion orbits strike the divertor plate with shallow angles because the magnetic field lines intersect the plate at a small angle. The neutralized atoms are emitted from the plate preferentially in one poloidal direction. The preferred direction, determined by the polarity of the toroidal magnetic field, agrees with experimental observation. © 1999 Elsevier Science B.V. All rights reserved.

Keywords: Divertor; Divertor simulation; Drifts; Neutral transport

1. Introduction

In–out asymmetry of divertor plasmas is observed in many experiments [1]. In single-null divertor configuration, more power is deposited on the electron side (for B clockwise as seen from the top; ion grad-B drift is toward the X-point located on the bottom, the electron side corresponds to the outboard divertor channel), and for the particle flux and electron pressure, the ion side is favored over the electron side. Switching toroidal field reverses the in–out asymmetry. This issue is particularly important in the divertor design of present and future high power devices, where the engineering margin for the heat flux is small, and helium ash must be pumped out efficiently. This issue is also related to divertor detachment, since detachment occurs first in the divertor channel with higher particle flux and lower heat flux.

In low density discharges, inner and outer heat fluxes are similar to within a factor of two. In moderate and higher densities, the increase of the radiated power in the ion-side channel reduces the power deposited on the ion side, enhancing the in–out divertor asymmetry. Actually, JT-60U experiments show that the sum of power deposited on the divertor plate and power radiated is in–out symmetric [2]. This in–out asymmetry and its reversal with B field reversal can be qualitatively explained by a classical effect [3]. Parallel ion force balance along the sol field lines requires a parallel electric field to compensate the thermal force along the field. Given the rotational transform and toroidal symmetry, parallel electric field gives rise to a poloidal electric field, which drives a radial particle $E \times B$ drift, which is in–out asymmetric.

In this paper, we offer an additional effect which may lead to the asymmetry. Ion particles hit the divertor plate at a shallow angle. The neutral particles are emitted from the divertor plate with a preferential poloidal direction, which tends to make the particle recycling flux in–out asymmetric. In Section 2, we present a simple analysis of ion gyration motion. In Section 3, we discuss the impact of the ion gyration motion on the reflection angle of the recycling neutrals. In Section 4, the asymmetry of density and temperature is discussed. The conclusions are summarized in Section 5.

* Corresponding author. Tel.: +81 292 82 5111; fax: +81 292 95 1549; e-mail: shimada@jaeri.go.jp.

[1] University of California, San Diego.

0022-3115/99/$ – see front matter
PII: S 0 0 2 2 - 3 1 1 5 (9 8) 0 0 6 7 9 - 5

2. Gyration motion of ion

The plasma ions strike the divertor plates and come back into the plasma as neutral atoms. The incident angle of the ions on the divertor plate depends on the angle between the magnetic field line and the divertor plate and also on the sheath potential drop between the plasma and the divertor plate.

We discuss the movement of gyration motion of ions and neutral particles in a coordinate system described in Fig. 1. In this coordinate system, z axis is taken along the toroidal field. $y = 0$ corresponds to the surface of the divertor plate. x axis is taken along the major radius (R). The field line intersects the divertor plate at an angle θ, which is usually very small (<0.1 radian). Here, $B_x = 0$ is assumed. A gyration motion of an ion incident on a divertor plate is described in Fig. 2. We take the direction of B field as $B > 0$; clockwise as seen from the top. All the coordinates are normalized to the ion Larmor radius. When the ion hits the divertor plate ($y = 0$), the velocity in the x direction is always negative with $B > 0$ and positive with $B < 0$.

Next we discuss the incident angle quantitatively. The geometry is described in Fig. 3. An ion enters the sheath at an angle α, then is accelerated by the sheath electric field, perpendicular to the surface. The incident angle is accordingly modified to β. The angle α of the ion incident on the sheath is dependent on the phase of the gyration motion. α is given by

$$\alpha = \tan^{-1}\left\{ \frac{|v_y|}{\sqrt{v_x^2 + v_z^2}} \right\} \approx 2\sqrt{\frac{\pi v_\perp v_\parallel \theta}{v_\perp^2 + v_\parallel^2}} \left(1 - \frac{\omega \Delta}{2\pi v_\parallel \theta}\right)^{\frac{1}{2}}, \quad (1)$$

where v_x, v_y, v_z are the velocity in the x, y and z direction, $v_\perp$ and $v_\parallel$ are the velocity perpendicular and parallel to the magnetic field line, Δ is the minimum value of y at the gyration period 1 cycle prior to the hitting event, and ω is the ion cyclotron frequency. Δ takes a value in the following range:

$$0 < \Delta \leqslant \frac{2\pi v_\parallel \theta}{\omega}. \quad (2)$$

Then the average α is approximately given by

$$\langle \alpha \rangle \approx \frac{4}{3}\sqrt{\frac{\pi v_\perp v_\parallel \theta}{v_\perp^2 + v_\parallel^2}} = \frac{4}{3}\left(\frac{\pi\theta}{3T_\mathrm{i} + T_\mathrm{e}}\right)^{\frac{1}{2}} (2T_\mathrm{i}(T_\mathrm{i} + T_\mathrm{e}))^{\frac{1}{4}} \quad (3)$$

where

$$v_\perp = \sqrt{\frac{2T_\mathrm{i}}{m}}, \quad (4)$$

$$v_\parallel = \sqrt{\frac{T_\mathrm{i} + T_\mathrm{e}}{m}} \quad (5)$$

are used (m is ion mass). For $T_\mathrm{i} = 3T_\mathrm{e}$,

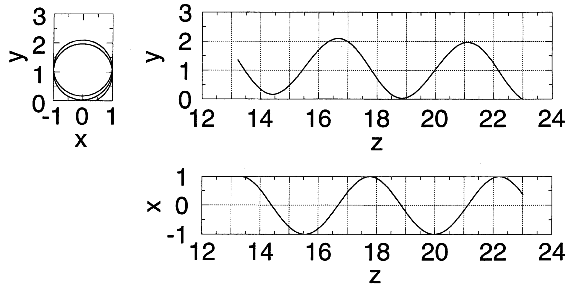

Fig. 2. Gyration motion of an ion prior to hitting a divertor plate. All the coordinates are normalized by the ion Larmor radius. When the ion hits the divertor plate ($y = 0$), the velocity in the x direction is always negative with $B > 0$ and positive with $B < 0$.

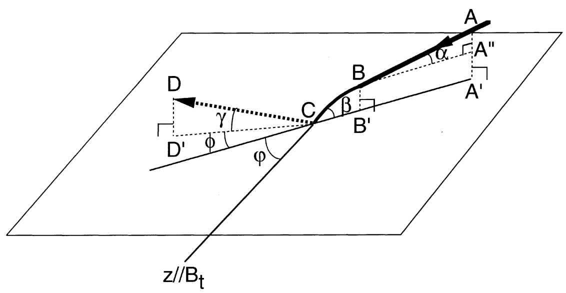

Fig. 3. Orbit of incident ion (ABC) and backscattered particle (CD). An ion enters the sheath at a shallow angle α, then is accelerated by the sheath potential, hitting the divertor plate ($y = 0$) at an angle β. The particle is then backscattered at an angle γ from the surface and at azimuthal angle ϕ measured from the line A′C. The angles are defined in the figure. The points A′, B′, D′ are the projection of points A, B and D to the divertor plate ($y = 0$ plane).

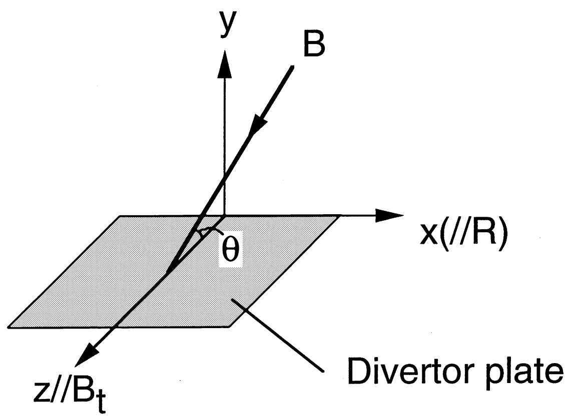

Fig. 1. Coordinate system used in this paper. The z axis is taken along the toroidal field. For simplicity, $B_x = 0$ is assumed. $y = 0$ corresponds to the surface of the divertor plate. x axis is taken along the major radius (R). The field line intersects the divertor plate at an angle θ.

$$\langle\alpha\rangle \approx 1.65\sqrt{\theta} \tag{6}$$

For $\theta = 0.03$ radian, $\langle\alpha\rangle \approx 0.286$ radian (16.4°).

Now we consider the effect of the sheath potential drop. We are in the regime

$$\rho_e \leqslant \lambda_D \ll \rho_i$$

where ρ_e and ρ_i are the gyro-radii of the electron and the ion and λ_D is the Debye length. We assume that the electrons reach the plate along the magnetic field lines, and the ions are accelerated by the sheath potential Ψ and strike the plate. The incident angle β of the ion hitting the divertor plate after the sheath acceleration is given by

$$\begin{aligned}\beta &= \tan^{-1}\left\{\sqrt{\frac{v_y^2 + 2\Psi/m}{v_x^2 + v_z^2}}\right\} \\ &= \tan^{-1}\left\{\sqrt{\frac{2\Psi/m}{v_\perp^2 + v_\parallel^2}\left(1 + \frac{2\pi v_\perp v_\parallel \theta - \omega v_\perp \Delta}{2\Psi/m}\right)}\right\}\end{aligned} \tag{7}$$

Averaging over Δ, we obtain the average β, which is given by

$$\langle\beta\rangle \approx \tan^{-1}\left\{\sqrt{\frac{2\Psi/m}{v_\perp^2 + v_\parallel^2}\left(1 + \frac{\pi v_\perp v_\parallel \theta}{2\Psi/m}\right)}\right\}. \tag{8}$$

Using $\Psi \approx 3T_e$, Eqs. (4) and (5), we obtain

$$\langle\beta\rangle \approx \tan^{-1}\left\{\sqrt{\frac{6T_e}{3T_i + T_e}\left(1 + \frac{(2T_i(T_i + T_e))^{1/2}}{6T_e}\pi\theta\right)}\right\} \tag{9}$$

$\langle\beta\rangle$ decreases for higher ratios of T_i/T_e. For $T_i = 3T_e$, and $\theta = 0.03$ radian, $\langle\beta\rangle = 0.695$ radian (39.8°). For $T_i = T_e$, and $\theta = 0.03$ radian, $\langle\beta\rangle = 0.901$ radian (51.6°).

The azimuthal angle φ can be given as follows:

$$\tan\varphi = \frac{v_x}{v_z} \approx \frac{v_\perp}{v_\parallel} = \sqrt{\frac{2T_i}{T_i + T_e}}. \tag{10}$$

For $T_i = 3T_e$, $\varphi = 0.886$ radian (50.8°).

3. Neutral particle reflection

When the ions impact the surface at a grazing angle, the energy perpendicular to the plate is very small. The parallel energy is little affected by the impact and the reflection is close to being specular. A substantial fraction of the ions picks up electrons from the surface and is reflected as neutral atoms. The ions reflected as ions will undergo similar impacts subsequently and are eventually neutralized.

The distribution function of backscattered particles can be calculated by the method proposed by Eckstein [4]. The energy, polar angle ($\pi/2 - \gamma$) and azimuthal angle ϕ of the reflected particles as well as reflection probability are calculated from a table generated from TRIM calculation. The azimuthal angle of the reflected neutral is given with respect to the azimuthal angle φ of the incident particle (Fig. 3), which can be converted to the azimuthal angle of the reflected neutral velocity with respect to the x axis.

Fig. 4 shows the distribution function $f(E)$ of backscattered particles directed inward and outward in the x direction, calculated for the condition of the incident particle: deuterium, target material: carbon, incident energy: 100 eV, incident angle: 30° from the surface. The asymmetry becomes significant toward higher energies. The ratio of particle flux backscattered inward to particle flux backscattered outward is 1.92. From $f(E)$, one can calculate the total particle fluxes F backscattered inward (Eq. (11)) and outward (Eq. (12)):

$$F_{v_x<0} = \int f_{v_x<0}(E)\,\mathrm{d}E, \tag{11}$$

$$F_{v_x>0} = \int f_{v_x>0}(E)\,\mathrm{d}E. \tag{12}$$

The sum of $F_{v_x<0}$ and $F_{v_x>0}$ equals the total backscattering (reflection) probability.

The asymmetry of backscattered fluxes F becomes even more pronounced with shallower incident angles (Fig. 5) and becomes lower with higher incident energies (Fig. 6). The total backscattered fluxes become larger with shallower incident angles (Fig. 5) and becomes lower with higher incident energies (Fig. 6). Fig. 7 shows asymmetry of total backscattered particle flux ($F_{v_x<0} -$

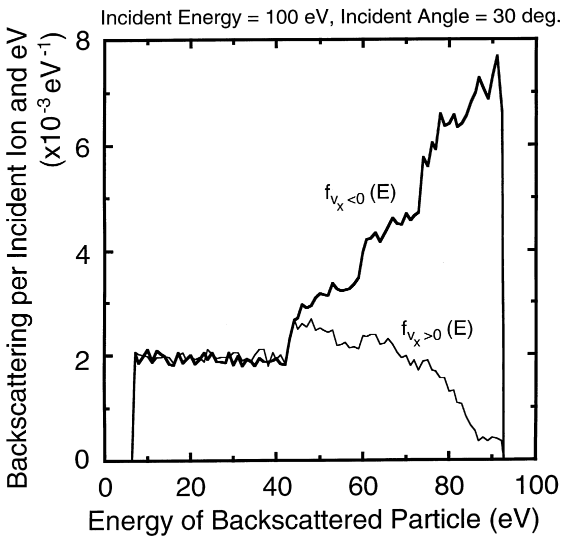

Fig. 4. Distribution functions of particles backscattered inward $f_{v_x<0}(E)$ and outward $f_{v_x>0}(E)$ are shown as a function of energy of backscattered particle. The asymmetry becomes significant toward higher energies. The incident particle: deuterium, target material: carbon, incident energy: 100 eV, incident angle: 30° from the surface. $T_i/T_e = 3$ is assumed.

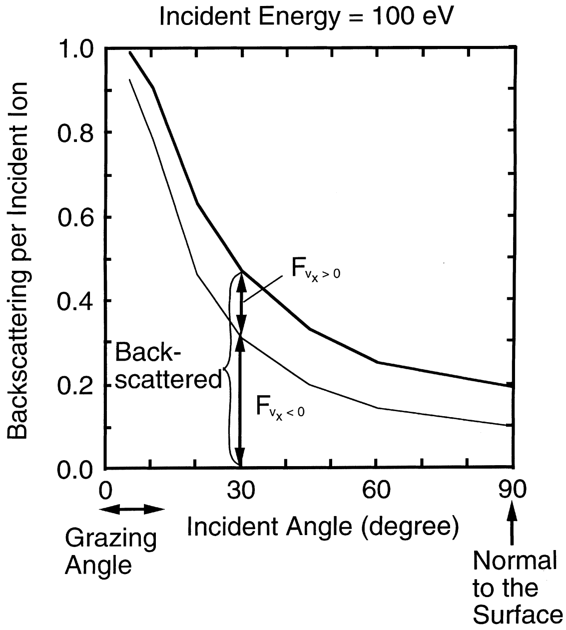

Fig. 5. Backscattered particle fluxes for different incident angles and fixed incident energy (100 eV). The thin line shows the particle flux backscattered inward $F_{v_x<0}$. The thick line shows the total backscattered particle flux. The difference between the thick and thin lines represents the particle flux backscattered outward $F_{v_x>0}$. $T_i/T_e = 3$ is assumed.

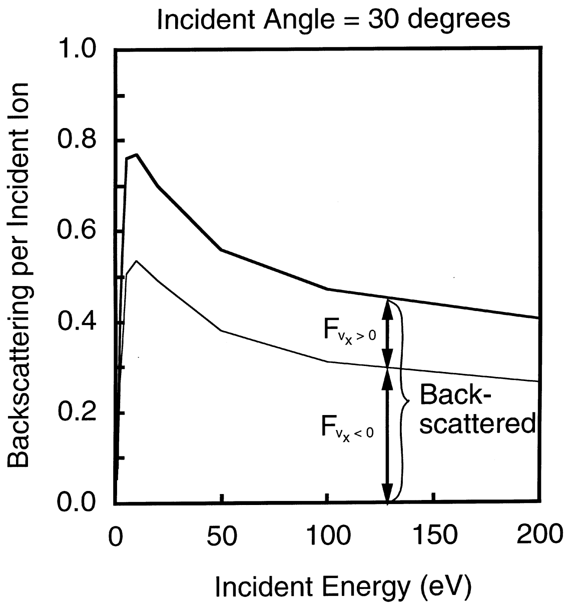

Fig. 6. Backscattered particle fluxes for different incident energies and fixed incident angle (30°). The thin line shows the particle flux backscattered inward $F_{v_x<0}$. The thick line shows the total backscattered particle flux. The difference between the thick and thin lines represents the particle flux backscattered outward $F_{v_x>0}$. $T_i/T_e = 3$ is assumed.

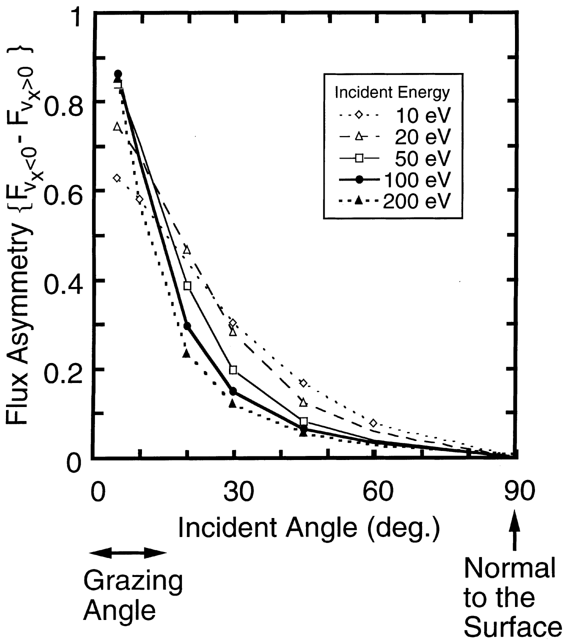

Fig. 7. Flux asymmetry of backscattered particle $(F_{v_x<0} - F_{v_x>0})$ as a function of incident angle and energy. This flux asymmetry can be regarded as that of total recycling particle flux (backscattering +reemission), as the particles not backscattered can be assumed to be reemitted isotropically. $T_i/T_e = 3$ is assumed.

$F_{v_x>0})$ as a function of incident angle and energy. Generally, flux asymmetry becomes more significant with shallower incident angles (ion temperature much higher than electron temperature) and lower incident energies. For the case of Fig. 4, the total flux of backscattered particle is 0.47 times the incident flux. In the steady-state, the particles that are not backscattered will be reemitted as thermalized particles; these particles can be assumed to be reemitted isotropically, and does not contribute to flux asymmetry. Therefore, the flux asymmetry of backscattered particles in Fig. 7 can be regarded as the asymmetry of total recycling particles.

The above analysis indicates that the recycling neutrals from the divertor plate are directed in a preferred poloidal direction. If the divertor plate is horizontal in a single null divertor, the direction is from outboard to inboard when the ion grad-B drift is toward the divertor. The opposite is true for the opposite polarity of the toroidal magnetic field. The asymmetry predicted from this theory agrees with experimental observation.

4. Discussion

We consider a 1-D sol. At the ends, the particle loss is nv_s which matches the recycling neutral flux Γ. Along the magnetic field line the pressure is approximately constant, implying that if there is a flow, it is subsonic. For the symmetric case, $n_1 v_{s1} = \Gamma_1 = \Gamma_2 = n_2 v_{s2}$ and $n_1 T_1 = n_2 T_2$, which leads to $n_1 = n_2$ and $T_1 = T_2$, where n is density, v_s is sound velocity and suffixes 1 and 2 denote inboard and outboard divertor, respectively. Suppose that the particle recycling is asymmetric, i.e. $\Gamma_1 = \Gamma_0$ $(1 + g)$ and $\Gamma_2 = \Gamma_0$ $(1 - g)$. The directed transport of the neutrals is represented by g. The solution is $T_2/T_1 = n_1/n_2 = (1 + g)^2/(1 - g)^2$. For example, if $g = 0.2$, then $T_2/T_1 = n_1/n_2 = 2.25$. This shows that a small asymmetry of particle recycling causes a significant asymmetry in density and temperature.

In this paper we have not discussed the effect of charge exchange or ionization of backscattered particles. As Fig. 4 shows, flux asymmetry is more significant toward higher energies. This means that the asymmetry of the particle source is more enhanced over the values shown in Fig. 7, since energetic particles have more probability of escaping the outboard divertor channel and reaching the inboard divertor channel and vice versa.

Recently, JT-60U has modified its divertor geometry [5]. In the new divertor, a divertor dome in the private flux region separates the two divertor channels. Particle flux asymmetry is still observed in experiments with a dome, suggesting that there is a strong mechanism driving asymmetry in addition to the gyromotion effect described in this paper.

5. Conclusion

A simple analysis of ion gyration motion indicates that ion orbits strike the divertor plate with shallow angles with a definite poloidal direction. The recycling neutral particles are emitted from the plate preferentially in one poloidal direction, determined by the polarity of the toroidal magnetic field. The preferred direction agrees with experimental observation. A quantitative assessment of this effect was made with a simple orbit model, and a particle backscattering model based on TRIM calculation. This effect becomes more significant with shallower angles (higher ratios of T_i/T_e) and lower incident energies.

Acknowledgements

The authors wish to express their gratitude to Drs W. Eckstein and D. Reiter, who provided them a database for particle reflection calculation. One of the authors (M.S.) would like to acknowledge fruitful discussion with Drs T. Takizuka and M. Sugihara.

References

[1] C.S. Pitcher, P.C. Stangeby, Plasma Phys. Control. Fusion 39 (1997) 779.
[2] N. Asakura et al., Plasma physics and controlled nuclear fusion research, (15th Conf. Proc., Seville, 1994), vol. 1, IAEA, Vienna, 1995, p. 515.
[3] F.L. Hinton, G.M. Staebler, Nucl. Fusion 29 (1989) 405.
[4] W. Eckstein, D.B. Heifetz, J. Nucl. Mater. 145 (1987) 332.
[5] N. Hosogane et al., these Proceedings.